EUROPEAN ORGANIZATION FOR NUCLEAR RESEARCH
European Laboratory for Particle Physics

*Large Hadron Collider Project*

**LHC Project Report 965**

# DESIGN OF THE LHC BEAM DUMP ENTRANCE WINDOW

R. Veness[1], B. Goddard[1], L. Massidda[2], S.J. Mathot[1], A. Presland[1]

## Abstract

7 TeV proton beams from the LHC are ejected through a 600 m long beam dump transfer line vacuum chamber to a beam dump block. The dump block is contained within an inert gas-filled vessel to prevent a possible fire risk. The dump vessel and transfer line are separated by a 600 mm diameter window, which must withstand both the static pressure load and thermal shock from the passage of the LHC beam. In a previous paper [1] the functional requirements and conceptual design of this window were outlined. This paper describes the analysis leading to the final design of the window. The choice of materials is explained and tests performed on the prototype window are summarized.

1 CERN, Geneva, Switzerland
2 CRS4, Pula, Italy

Presented at the Tenth European Particle Accelerator Conference (EPAC'06)
26-30 June 2006, Edinburgh, UK

CERN
CH - 1211 Geneva 23
Switzerland

Geneva, 4 August 2006

# DESIGN OF THE LHC BEAM DUMP ENTRANCE WINDOW

R. Veness, B. Goddard, S.J. Mathot, A. Presland, CERN, Geneva, Switzerland
L. Massidda, CRS4, Pula, Italy

*Abstract*

7 TeV proton beams from the LHC are ejected through a 600 m long beam dump transfer line vacuum chamber to a beam dump block. The dump block is contained within an inert gas-filled vessel to prevent a possible fire risk. The dump vessel and transfer line are separated by a 600 mm diameter window, which must withstand both the static pressure load and thermal shock from the passage of the LHC beam. In a previous paper [1] the functional requirements and conceptual design of this window were outlined. This paper describes the analysis leading to the final design of the window. The choice of materials is explained and tests performed on the prototype window are summarized.

## INTRODUCTION

The window must maintain the required pressure differential, and also cope with both the repeated dynamic thermal load when the ultimate intensity LHC beam ($4.8\times10^{14}$ protons at 7 TeV) is dumped, together with the worst-case thermal load which could happen if the dilution kicker system fails, either partially or totally and the full LHC beam is swept over a much shorter length, with a correspondingly higher energy density. The loss of vacuum tightness in extreme accident cases is acceptable; however, the window must retain its structural integrity under all load conditions. The conceptual and mechanical designs have been based on FLUKA energy deposition simulations, together with numerical and analytical stress calculations, in particular estimates of dynamic effects which are computationally difficult. The mechanical design has also been constrained by the window size and materials, which condition the available methods.

## CONCEPTUAL DESIGN

The basic concept [1] was to use a carbon-carbon (C-C) composite window. The SIGRABOND 1501G grade from SGL was selected, taking advantage of the combination of transparency to particles, good high-temperature mechanical strength, elastic modulus and temperature resistance. C-C composites are relatively porous ($5\times10^{-2}$ mbar.l.s$^{-1}$.cm$^{-2}$ permeation for the grade selected), so a single composite wall would require an unrealistic pumping speed of 40 m$^3$h$^{-1}$ to achieve the required vacuum of $1\times10^{-6}$ mbar. A differential pumping system with two C-C walls and an intermediate low-vacuum mechanical pump was considered, but rejected due to the mechanical complexity in the radioactive environment. A thin leak-tight layer was thus added.

Despite their porosity, unbaked C-C sheets can achieve low outgassing rates in the order of $5\times10^{-11}$ mbar.l.s$^{-1}$.cm$^{-2}$ after 100 h pumping [2] due to their graphitization cycle at above 2000 ºC. The leak-tight layer was therefore put on the high pressure side, to avoid risk of delamination. A sputtered or electro-deposited coating was considered, but tests at CERN have shown no success in producing leak-tight layers due to the open structure of the composite, so a separate mechanical foil was chosen, welded for reliability.

As the foil is fully supported by the C-C sheet, the main load will be thermo-elastic stress $\sigma_t$ due to the passage of the beam. A figure of merit, X, for material m compared with 316L stainless steel can be established:

$$X = \frac{\sigma_t^{316L}}{\sigma_t^m} = \frac{E^{316L}\alpha^{316L}}{E^m\alpha^m}$$

Where E is the elastic modulus and $\alpha$ the linear coefficient of thermal expansion. Using data for potential materials gives values for X in Table 2.

Table 1: Figures of merit for potential foil materials

| | 316L | Aluminium | Titanium | Beryllium |
|---|---|---|---|---|
| $T_{fusion}$(K) | 1700 | 933 | 1948 | 1550 |
| X | 1 | 2.0 | 3.2 | 0.93 |

Beryllium was shown to be non-optimal for this application due to it's high elastic modulus, aluminium was rejected due to the low fusion temperature, titanium was seriously considered, but rejected due to the availability of special wide foils and development time required for foil welding. A thin foil in a vacuum compatible stainless steel grade was therefore selected.

## FLUKA ANALYSIS

The energy deposition in the 15 mm CC plate and 200 μm steel foil was calculated with FLUKA [3] for a single 7 TeV LHC ultimate proton bunch, with a beam size (1 $\sigma$) of 1.6 mm and 1.4 mm in the H and V planes respectively. The total energy deposition was then calculated for the full beam in a post-processing routine where this pattern was superimposed 2808 times on the window mesh, using the nominal or failure sweep profile. The temperature rise $\Delta T$ was then calculated numerically using the temperature dependant heat capacity. The maximum temperature rise for the nominal sweep is 15 K in the CC, 42 K in the foil. For the total dilution failure, the maximum temperature increases are 891 K and 3580 K respectively.

## MECHANICAL DESIGN

The structure can be separated into discrete, superposable parts. The C-C sheet was considered to bear all the static pressure loading along with quasi-static and dynamic thermo-mechanical loads due to the beam passage. The thin foil was considered to be entirely supported by the C-C sheet and so only the quasi-static thermo-mechanical load was considered.

### *Static pressure loading*

The C-C sheet can be considered as a thin plate, simply supported around the circumference. Clearances are allowed such that differential thermal stresses due to the supports are not applied. Temperature-dependant, isotropic properties for the bulk material are given by the supplier. The pressure loading can therefore be analysed using analytical formulae for a thin plate under uniform pressure with small deflections [4].

Under a pressure of 0.14 MPa this analysis yields maximum radial stress of 69 MPa and a deflection of 2.9 mm for a 15 mm thick plate. Fluka analysis showed that the maximum temperature only increased by ~10 % compared with a plate of 10 mm thickness. It was therefore decided to err on the side of mechanical safety.

### *Thermo-elastic loading*

Detailed dynamic thermo-elastic analysis of these types of structures is extremely complex for a number of reasons: the C-C plate is, in reality, non-isotropic with significant differences in mechanical properties between the transverse and through-thickness directions; the beam size is small and produces a very local heating of the structure; finally, the beam passage is very rapid, producing a quasi-step increase in temperature and hence possible shock waves in the structure. To analyse this correctly would require details of the structural properties of the composite at the individual fibre level that are not available without extensive testing. It would also require a large, multi-step, finite element (FE) model.

In order to evaluate the justification for such a model, it was decided to make a simplified analysis, using analytical and FE analysis.

The three thermal cases considered in [1] can be simplified in the following way: The ‘nominal’ case where the beam is swept in a circle and ‘total kicker failure’ case where the beam passes as a point in the centre of the window can be considered as axisymmetric; the ‘single kicker failure’ case where the beam is swept on a line across the window is clearly a 2-D geometry. However, by assuming the window is quasi-infinite, a plain strain simplification can be made, allowing a linear cut across the beam path.

Finite element analysis was made for these simplified models using the ANSYS code and using the temperature profiles produced in the FLUKA analysis. Resultant values for the Von Mises equivalent stress in the 316L foil and C-C plate are given in Table 2.

For comparison, the maximum temperature from the FLUKA analysis was considered as an idealized thermal step $\Delta T$, and the corresponding thermo-elastic stress $E\alpha\Delta T$ computed for the materials with elastic modulus E and coefficient of thermal expansion $\alpha$.

Table 2: Results of stress analysis for different operational modes (Von Mises equivalent stress)

| **Case** | **Nominal** | | **Single failure** | | **Double failure** | |
|---|---|---|---|---|---|---|
| Material | C-C | 316L | C-C | 316L | C-C | 316L |
| Max. $\Delta T$ (K) | 15 | 42 | 170 | 540 | 910 | 3600 |
| ANSYS (MPa) | 1 | 121 | 9 | 1629 | 57 | - |
| Idealised step $\Delta T$ (MPa) | 1.1 | 134 | 11 | 1890 | 63 | - |

A number of conclusions can be drawn from table 2. The ANSYS and analytical models produce very similar results for all three cases. This confirms that the temperature profile used in the simplified ANSYS model represents, effectively, a step temperature change. This is not surprising considering the local nature of the beam passage. It suggests that static stresses can be closely approximated using this simple analytical model. The stresses in the C-C plate are low, even in the double failure case. This is because the bulk transverse coefficient of thermal expansion for the material is close to zero at room temperature, and only increases to $1\times10^{-6}\ K^{-1}$ at the peak temperature of 1203°C. Thus any thermal stress analysis based on these coefficients will yield low stresses.

The stress calculated in the stainless foil is ~60% of the yield stress for the nominal condition which can be considered acceptable. For the single kicker failure it is already three times the ultimate strength. For the total kicker failure, the foil will locally melt, so the stress is irrelevant.

### *Dynamic Analysis*

The dynamic stresses are related to the material properties, the maximum value of the temperature and its distribution, and the rate of the temperature increase: a short energy deposition time and large deposition area result in high values of the dynamic stress components.

The relative importance of the dynamic component of the stress may be evaluated by comparing the time required for the energy deposition to the time required to an elastic wave to travel trough the heated area.

A semi-analytical solution of this problem is available [5] for the case of stress waves in a thin disc of radius R, heated steadily with time to temperature T in time $t_0$ over a radius $r_0$. For a ‘long’ heat pulse, where the time taken for the pulse to travel through the heated area is less than the heating time, ie, $r_0 < c\ t_0$ (where $c = \sqrt{E/\rho}$ is the speed of sound in the material, E is the elastic modulus and ρ the density), then the contribution of the dynamic stress components $\sigma_r^{max}$ and $\sigma_\phi^{max}$ relative to the peak static thermo-elastic stresses $\overline{\sigma}_r$ and $\overline{\sigma}_\phi$ is given by

$$\frac{\sigma_r^{max}}{\overline{\sigma}_r} = \frac{\sigma_\phi^{max}}{\overline{\sigma}_\phi} \leq \frac{4r_0}{ct_0}$$

However, for a 'short' pulse where $r_0 >> c\ t_0$ then stress waves can superpose, and considerably higher dynamic stress contributions can occur.

Considering the present design where the heating time $t_0$ is 86 μs and the speed of the wave $c=7.5x10^3$ m.s$^{-1}$, then for the 'total failure' case, where $r_0$ =0.01m, the pulse can be considered 'long' and the contribution of the dynamic stress is ~1.5% of the static stress. For the nominal and 'single failure' cases, an assumption must be made for the heated area. Taking the most pessimistic assumption that it is equal to the swept radius, then the pulse is still 'long', but the dynamic contribution could rise to ~15% of the static stress.

## MANUFACTURE AND TEST

The foil was electron beam (EB) welded to the support flange with a cover plate to prevent local buckling. A wide, shallow weld was adopted to ensure leak-tightness (Fig. 1). The completed assembly (Fig. 2) was helium leak tight to below $5x10^{-11}$ Pa.m$^3$.s$^{-1}$. Deformation of the plate was measured to be 3.05 mm with a ΔP of 0.1 MPa, compared with the calculated value of 2.07 mm.

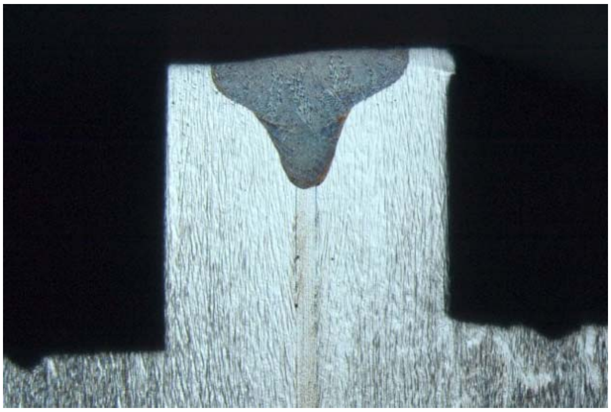

Figure 1: Micrograph showing the EB weld geometry

## CONCLUSIONS

The simplified static thermal analysis shows that the stresses can be closely approximated by idealised temperature steps. Due to the geometry of the window and temperature profile, dynamic stresses are unlikely to be significant.

The structure should withstand the passage of the ultimate LHC beam without degradation. Failure of a single kicker will cause significant plastic deformation of the thin foil which may then leak. Failure of both kickers will locally melt the foil. In either failure case, the C-C plate should maintain mechanical integrity.

Detailed dynamic thermo-elastic stress would be useful to understand the behaviour under the failure cases, but would be unlikely to lead to any change to the baseline design.

The performance of the window must also be verified with heavy ions, since the energy deposition over short distances is very different to protons.

Replacing the stainless foil with titanium would be a potential upgrade option. It would result in a reduction of a factor of 3.2 in the foil stress (see Table 1), which would allow the foil to resist the 'single kicker failure' case without plastic deformation.

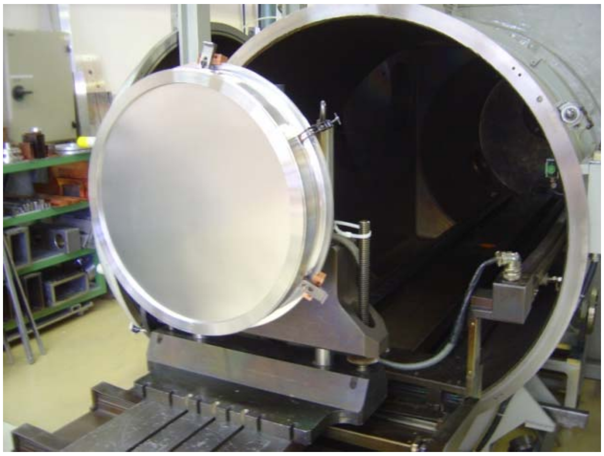

Figure 2: Window prototype in EB chamber

## ACKNOWLEDGEMENTS

The contributions of D .Duarte Ramos, L. Faisandel, A. Gerardin, J.M. Jimenez, T. Tardy, B. Versolatto and W. Weterings are gratefully acknowledged.

## REFERENCES

[1] A. Presland et al., "A Large Diameter Entrance Window for the LHC Beam Dump Line", PAC'05 Knoxville Tennessee, May 2005, p.1698

[2] T. Deville, B.Versolatto, "Mesures de Degassage de Composites Carbone-Carbone" CERN/LHC Vacuum Technical Note 98-22, 1998.

[3] A. Fasso et al., "FLUKA: Status and Prospective for Hadronic Applications", Proc. MonteCarlo 2000 Conference, Lisbon, 2001.

[4] W.C. Young 'Formulas for stress and strain', McGraw-Hill, 1989

[5] P. Sievers, "Elastic stress waves in matter due to rapid heating by an intense high-energy particle beam", CERN LAB II/BT/74-2 (1974)